

DOE/BC/14994-19
(OSTI ID: 13828)

OPTIMIZATION OF FLUID FRONT DYNAMICS IN POROUS MEDIA
USING RATE CONTROL: I. EQUAL MOBILITY FLUIDS

Topical Report
August 1999

By
Bagus Sudaryanto
Yanis C. Yortsos

Date Published: October 1999

Work Performed Under Contract No. DE-FG22-96BC14994/SUB

University of Southern California
Los Angeles, California



National Petroleum Technology Office
U. S. DEPARTMENT OF ENERGY
Tulsa, Oklahoma

DISCLAIMER

This report was prepared as an account of work sponsored by an agency of the United States Government. Neither the United States Government nor any agency thereof, nor any of their employees, makes any warranty, expressed or implied, or assumes any legal liability or responsibility for the accuracy, completeness, or usefulness of any information, apparatus, product, or process disclosed, or represents that its use would not infringe privately owned rights. Reference herein to any specific commercial product, process, or service by trade name, trademark, manufacturer, or otherwise does not necessarily constitute or imply its endorsement, recommendation, or favoring by the United States Government or any agency thereof. The views and opinions of authors expressed herein do not necessarily state or reflect those of the United States Government.

This report has been reproduced directly from the best available copy.

DOE/BC/14994-19
Distribution Category UC-122

Optimization of Fluid Front Dynamics in Porous Media
Using Rate Control: I. Equal Mobility Fluids

By
Bagus Sudaryanto
Yanis C. Yortsos

October 1999

Work Performed Under Contract DE-FG22-96BC14994/SUB

Prepared for
U.S. Department of Energy
Assistant Secretary for Fossil Energy

Thomas B. Reid, Project Manager
National Petroleum Technology Office
P.O. Box 3628
Tulsa, OK 74101

Prepared by
Petroleum Engineering Program
Department of Chemical Engineering
University of Southern California
Los Angeles, CA 90089-1211

TABLE OF CONTENTS

Abstract	v
Introduction	1
I. Homogeneous Porous Media	3
<u>1. Formulation</u>	3
<u>2. Computational Procedure</u>	7
<u>3. Numerical Results</u>	8
<u>4. Constraint on Injectivity</u>	11
<u>5. Experimental Results</u>	12
II. Heterogeneous Porous Media	14
<u>1. Formulation</u>	15
<u>2. Numerical Results</u>	17
<u>3. A Sensitivity Study</u>	18
<u>4. Experiments</u>	19
Conclusions	20
Acknowledgements	21
Figures	25-43

Abstract

In applications involving the injection of a fluid in a porous medium to displace another fluid, a main objective is the maximization of the displacement efficiency. For a fixed arrangement of injection and production points (sources and sinks), such optimization is possible by controlling the injection rate policy. Despite its practical relevance, however, this aspect has received scant attention in the literature. In this paper, we provide a fundamental approach based on optimal control theory, for the case when the fluids are miscible, of equal viscosity and in the absence of dispersion and gravity effects. Both homogeneous and heterogeneous porous media are considered. From a fluid dynamics viewpoint, this is a problem in the deformation of material lines in porous media, as a function of time-varying injection rates. It is shown that the optimal injection policy that maximizes the displacement efficiency, at the time of arrival of the injected fluid, is of the “bang-bang” type, in which the rates take their extreme values in the range allowed. This result applies to both homogeneous and heterogeneous media. Examples in simple geometries and for various constraints are shown, illustrating the efficiency improvement over the conventional approach of constant rate injection. In the heterogeneous case, the effect of the permeability heterogeneity, particularly its spatial correlation structure, on diverting the flow paths, is analysed. It is shown that “bang-bang” injection remains the optimal approach, compared to constant rate, particularly if they were both designed under the assumption that the medium was homogeneous. Experiments in a homogeneous Hele-Shaw cell are reported to test the theory.

Introduction

The injection of a fluid in a porous medium to displace another fluid (miscible or immiscible) initially in place is common to applications involving the recovery of subsurface fluids (for example, in oil recovery or in environmental soil remediation). Injected fluids are typically water, solvents, steam, etc., the initial fluid being oil or organic contaminants, in the two applications mentioned. The displacement occurs by injection from various injection wells (sources) and by production from a number of production wells (sinks). A variety of patterns have been analyzed in classical works (e.g. Muskat¹, Bear²), several decades ago. A typical example of relevance to our work, is shown in Figure 1 and involves two injection wells and a production well in a bounded “reservoir”. In practice, the location of injection and production wells is generally determined semi-empirically, based on a variety of geologic, economic, and practical considerations.

In many applications, the main objective is the maximization of some measure of the displacement efficiency (the recovery efficiency). Aspects of the optimization of displacement processes in porous media have been studied before, notably by Ramirez and his co-workers³⁻⁷, in the context of maximizing the profitability over a fixed time interval of various Enhanced Oil Recovery (EOR) processes. In these, the important variable is the volume of a (costly) component (e.g. surfactant, polymer) injected along with the fluid, which improves the microscopic (pore-level) displacement efficiency. There, the emphasis is mostly on the physicochemical action of the injected fluid (for instance, on the reduction of the interfacial tension) rather than on the dynamics of the flow itself. Typically, in those studies, a pair of injection and production wells in a symmetric, homogeneous pattern were considered.

However, in problems where the injected fluid composition is fixed and it is not a control parameter (for example in water displacing oil), the only available control of the displacement is the allocation of the injected fluid to the injection wells (and of the produced fluid to the production wells). In general, this can be accomplished by varying the injection rates and/or the injection (or production) intervals in individual wells. In the particular case of a 2-D geometry of interest here, the wells can be considered as point sources and sinks, thus the maximization of the displacement efficiency should be sought by optimizing well injection

rates. This fundamental problem has not been systematically addressed before (although various attempts have been made, e.g. see Asheim⁸ and Virnovsky⁹). The conventional approach has been to design symmetric well patterns, and allocate injection rates equally to all wells. This practice relies on the premise that the permeability field is homogeneous, an assumption which is rarely true. Indeed, in heterogeneous porous media, the flow streamlines do not necessarily have the symmetry of the well pattern, even at constant injection rates. Furthermore, injection at constant and equally partitioned rates, which is a common practice, has not been shown to be the optimal policy, certainly not in the absence of well symmetry, even for a homogeneous porous medium.

To make progress, we elected to study in this paper a “first-order” problem, namely equal-viscosity, first-contact miscible displacement, in two dimensions and in the absence of dispersion or gravity. In the case of a homogeneous permeability field, this, then, becomes a problem of control of fluid fronts under conditions of potential flow. As will be shown below, this problem is amenable to a non-linear dynamics description. For heterogeneous permeability fields, a similar although computationally more complex, description applies. Accounting for the presence of dispersion, of immiscible fluids and of unequal viscosities, which are all neglected here, introduces additional complexities. For example, when the fluids are immiscible, issues of relative permeabilities arise. While in the case of a less viscous fluid displacing a more viscous one, viscous fingering instabilities will occur^{10–13}, requiring a generally cumbersome numerical approach, instead of the simpler potential flow description used here. Some of these more general problems are discussed in a companion paper¹⁴, which relies, however, on the present approach for their solution.

From a fluid dynamics point of view, the problem under consideration is the evolution of displacement fronts in porous media, as a function of time-varying injection rates at point sources. In essence, this is a study of the deformation (map) of initial material lines subject to a time-varying flow field (for example, as described in Ottino¹⁵). Given that 2-D steady-state potential flow is integrable¹⁵, it is the time dependence of the injection rates at discrete points (sources and sinks) that potentially introduces interesting aspects. The general problem of the deformation of arbitrary fluid volumes in various porous media flow fields is discussed elsewhere¹⁶ and will form the subject of a future article. In this paper, the focus is on how to

control the displacement fronts to optimize a certain measure of the displacement. For the latter, we select the displacement efficiency at the time when the injected fluid first arrives (“breaks through”) at the production well. Delaying as much as possible the arrival of the injected fluid at the production well is a desirable objective in many recovery processes. We note that interesting work on the arrival time statistics in heterogeneous porous media has been recently carried out¹⁷.

Thus, we consider the equal-mobility, miscible displacement of incompressible fluids in a 2-D geometry in the absence of dispersion and gravity. For the sake of presentation, we will refer to the injected fluid as “water” and to the displaced fluid as “oil”, without any particular physicochemical meaning attached to this designation, however. The paper is organized in two sections, as follows: First, we formulate the control problem in a homogeneous permeability field, involving multiple injectors and one producer. We apply an optimal control methodology and show that the optimal control policy is of the “bang-bang” type, namely, the control parameter, which here is the injection rate at individual point sources, takes only its extreme values (maximum or minimum) in the range in which they are constrained. Numerical experiments are subsequently conducted to illustrate the applicability of the methodology and to carry out a sensitivity study. Then, we report on physical flow experiments conducted in a Hele-Shaw cell to test the theoretical predictions. In the second section of the paper, we present a generalization of the approach to heterogeneous reservoirs, always under conditions of equal mobility, and conduct a sensitivity study of the effect of heterogeneity on the optimal injection policy.

I. Homogeneous Porous Media

1. Formulation

Under the previous assumptions of equal mobility, incompressible miscible fluids, and in the absence of dispersion and gravity effects, the displacement in homogeneous porous media is governed by potential flow

$$\nabla^2\Phi = 0 \tag{1}$$

where Φ is a normalized flow potential. The solution of (1) for a multiple-well, multiple-rate problem in 2-D reads, in appropriate dimensionless notation, as

$$\Phi(x, y) \sim - \sum_{l=1}^{N_T} q_l(t) \ln \left[(x - x_{wl})^2 + (y - y_{wl})^2 \right] \quad (2)$$

where N_T is the total number of wells, q_l is the flow rate of well l ($q_l \geq 0$ for injection and $q_l \leq 0$ for production), and the pair (x_{wl}, y_{wl}) denotes the coordinates of well l . Throughout the paper, sources are not allowed to become sinks, and vice versa. We add that in the case of bounded symmetric reservoirs, N_T also includes the image wells present as a result of the method of superposition.

From equation (2) and the use of Darcy's law, the flow velocities read, in appropriate dimensionless notation

$$v_x = \sum_{l=1}^{N_T} q_l(t) \left[\frac{x - x_{wl}}{(x - x_{wl})^2 + (y - y_{wl})^2} \right] \quad (3)$$

and

$$v_y = \sum_{l=1}^{N_T} q_l(t) \left[\frac{y - y_{wl}}{(x - x_{wl})^2 + (y - y_{wl})^2} \right] \quad (4)$$

Equations (3)-(4) can also be used to define fluid fronts by tracking front particles emanating from the various sources. With this description, the optimization problem can be formulated as an optimal control problem of a non-linear dynamical system. Define as state variables the coordinates (x_k, y_k) of the (theoretically infinite) particles at the fronts. Then, the state equations are

$$\dot{x}_k = \sum_{l=1}^{N_T} q_l(t) \left[\frac{x_k(t) - x_{wl}}{(x_k(t) - x_{wl})^2 + (y_k(t) - y_{wl})^2} \right] \quad (5)$$

and

$$\dot{y}_k = \sum_{l=1}^{N_T} q_l(t) \left[\frac{y_k(t) - y_{wl}}{(x_k(t) - x_{wl})^2 + (y_k(t) - y_{wl})^2} \right] \quad (6)$$

where dots denote differentiation with respect to time, subject to the initial conditions $x_k(0) = x_k^0$ and $y_k(0) = y_k^0$. The latter are determined by specifying the particular source

and the particular streamline angle from which the particle emanated (recall the locally radial flow near a source or a sink).

In this dynamical system, the control variables are the time-varying injection rates $q_l(t)$. These are subject to various constraints. For example, consider the case in which there is a single sink, denoted by subscript 1, and $N_W - 1$ sources. A plausible constraint is to assume that the overall injection rate is constant, and equal to 1, in the dimensionless notation, in which case we have the conditions

$$q_1(t) = -1 \quad , \quad \sum_{l=2}^{N_W} q_l(t) = 1 \quad , \quad 0 \leq q_l(t) \leq 1 \quad , \quad l = 2, \dots, N_W \quad (7)$$

Other constraints are also possible, for example on the maximum possible rates in individual wells (see below and Ref. [16]). Now, for the case of incompressible fluids at a constant-overall injection rate, maximizing the efficiency at breakthrough is equivalent to maximizing the breakthrough (arrival) time, t_f . In this case, therefore, the performance index \mathcal{J} to be maximized is

$$\mathcal{J} = t_f \quad (8)$$

The arrival time is determined from the solution of the state equations. In the numerical approximation to be used below, the front will be approximated by a finite number N_S of particles. Because of the singularity of flow near the sink, the following terminal condition will be imposed

$$\psi(t_f) \equiv \prod_{k=1}^{N_S} \left([x_k(t_f) - x_w1]^2 + [y_k(t_f) - y_w1]^2 - \epsilon^2 \right) = 0 \quad (9)$$

where $\epsilon \ll 1$ is a normalized source “radius”. Thus, breakthrough is defined when condition (9) is satisfied for the first time, which occurs when the fastest particle, under the particular injection rate policy, first arrives at the sink.

In summary, the optimal control problem to be solved can be stated as follows: Find the admissible control parameters $q_l(t)$, $l = 2, \dots, N_W$, satisfying the constraints given by (7) which maximize the performance index (8), subject to the state equations (5)-(6) and the stopping criterion (9). This problem can be addressed by using a standard control

methodology¹⁸.

For this, we introduce the Hamiltonian,

$$\begin{aligned} \mathcal{H} = & \sum_{k=1}^{N_S} \lambda_{xk}(t) \left[\sum_{l=1}^{N_T} q_l(t) \left[\frac{x_k(t) - x_{wl}}{(x_k(t) - x_{wl})^2 + (y_k(t) - y_{wl})^2} \right] \right] \\ & + \sum_{k=1}^{N_S} \lambda_{yk}(t) \left[\sum_{l=1}^{N_T} q_l(t) \left[\frac{y_k(t) - y_{wl}}{(x_k(t) - x_{wl})^2 + (y_k(t) - y_{wl})^2} \right] \right] \end{aligned} \quad (10)$$

and adjoin the state equations (5)-(6) and the terminal condition (9) to the objective function (8), using the vector Lagrange multipliers $\lambda_{xk}(t)$ and $\lambda_{yk}(t)$ and the scalar Lagrange multiplier ξ . This leads to the augmented objective function

$$\mathcal{J}_A = t_f + \xi\psi + \int_0^{t_f} \left[\mathcal{H} - \sum_{k=1}^{N_S} (\lambda_{xk}(t)\dot{x}_k + \lambda_{yk}(t)\dot{y}_k) \right] dt \quad (11)$$

from which the Lagrange multipliers are determined

$$\dot{\lambda}_{xk} = -\frac{\partial \mathcal{H}}{\partial x_k} \quad \dot{\lambda}_{yk} = -\frac{\partial \mathcal{H}}{\partial y_k} \quad \text{and} \quad \xi^{-1} = - \left[\sum_{k=1}^{N_S} \left(\frac{\partial \psi}{\partial x_k} \dot{x}_k + \frac{\partial \psi}{\partial y_k} \dot{y}_k \right) \right]_{t_f} \quad (12)$$

subject to the boundary conditions

$$\lambda_{xk}(t_f) = \xi \left(\frac{\partial \psi}{\partial x_k} \right)_{t_f} \quad \text{and} \quad \lambda_{yk}(t_f) = \xi \left(\frac{\partial \psi}{\partial y_k} \right)_{t_f} \quad (13)$$

A computational procedure for the maximization of (11) will be described shortly. Before we proceed, however, we make a key observation: We note that the state equations (5)-(6) are *linear* with respect to the control parameters $q_l(t)$. Under these conditions, we can apply Pontryagin's Maximum Principle (PMP), which states that the optimal variable q_l^* is determined from the value of the switch function $\frac{\partial \mathcal{H}}{\partial q_l}$ as follows (e.g. see Bryson and Ho¹⁸): $q_l^* = q_{min}(= 0)$ if $\frac{\partial \mathcal{H}}{\partial q_l} < 0$; $q_l^* = q_{max}(= 1)$ if $\frac{\partial \mathcal{H}}{\partial q_l} > 0$; while q_l^* is undetermined if $\frac{\partial \mathcal{H}}{\partial q_l} = 0$. Therefore, if the values of the switch functions are non-zero, except possibly at a finite number of points, the optimal (non-singular) control is of the ‘‘bang-bang’’ type, and the control variables take their extreme values only (which in the present case are 0 and 1).

2. Computational Procedure

Because of the bang-bang control nature of the problem, therefore, we only need to specify the switch times and the control value of the first bang arc. The problem reduces into finding the optimum location of the switch times. Various algorithms^{19–22} have been proposed for this purpose. In this study, we will use the STO (switching time optimization) algorithm, developed by Meier and Bryson²², which is based on a first-order gradient method and consists of the following steps:

1. Obtain the initial switch time and the control value of the first-bang arc (see further below).
2. Using the initial control policy from step (1), integrate the state equations (5) and (6) forward in time until the stopping criterion (9) is satisfied. Record all state variables $x_k(t)$ and $y_k(t)$ ($k = 1, \dots, N_S$) and the value of the objective function.
3. Calculate the Lagrange multipliers $\lambda_{xk}(t)$, $\lambda_{yk}(t)$ ($k = 1, \dots, N_S$) and ξ from the co-state equations (12) by integrating backward in time, starting from the terminal time t_f and using the boundary condition (13).
4. Calculate the improvement in the switch time, dt_{lm} , by using the expression

$$dt_{lm} = \frac{w_{ll}}{\Delta q_l} \left(\frac{\partial \mathcal{H}}{\partial q_l} \right)_{t_{lm}} \quad (14)$$

where t_{lm} is the m -th switch time of the control variable q_l , w_{ll} is the diagonal element of a positive definite weight matrix W (see Ref. [16] for more details), and $\Delta q_l \equiv q_l(t_{ml}) - q_l(t_{ml} + dt_{ml})$ is here equal to $\Delta q_l = \pm 1$.

4. Repeat steps (2)-(4) using the new switch times obtained from step (4) until the change in the objective function is less than a prescribed small positive number.

To get started, the STO algorithm requires an initial guess of switch times (step (1)), which can be obtained by solving a modified non-bang-bang problem that approximates the original bang-bang problem²². In the modified problem, a term that approximates the control bounds must be added to the performance index. This term penalizes the deviation of the controls away from the bounds. Using the above gradient procedure (see ref. [16] for more details), the control parameters of the modified problem are driven toward their

bounds to maximize the performance index J . Results are presented below.

3. Numerical Results

All numerical results to be shown in this subsection correspond to a three-well system (two injectors and one producer) in a rectangular, bounded reservoir (Fig. 1). In the solution of the problem, we used the method of images by superposing image wells to satisfy the no-flow conditions at the boundaries (for example, see Refs. [1]-[2]). A total of seventy-two image wells was found to be numerically sufficient for this purpose. We note that a similar approach can also be implemented for arbitrary reservoir geometries¹⁶. The numerical experiments were typically conducted by fixing the positions of wells A and C, and of the angle $\alpha = \hat{A}CB$ and placing well B at variable positions. Of course, various other geometrical configurations are also possible. The following general results were found: In all cases under the constraint of constant-overall injection rate, only one injector (source) is active at any given time. (However, this is not necessarily the case for different constraints, as will be shown later.) The optimal injection policy is bang-bang with one switch time only: it consists of injecting first from the source well located “farther” away from the sink (well A in Fig. 1), up to the optimal switch time, at which injection switches to the injector located “nearest” to the producer (well B in Fig. 1). Furthermore, the optimal switch time was found to be such that the fronts from both injectors arrive simultaneously at the producer.

Snapshots of the displacement fronts under the optimal injection policy are shown in Fig. 1. Before the switch time, only injection from the point source A takes place (Fig. 1b). Following the switch, injection terminates at source A and commences at source B. The particles originating from source A are now subject to the flow field created by the source at point B, and they are displaced in the direction of the sink C (Fig. 1c). During this process, part of the front emanating from source A recedes, although the total volume it encloses remains constant, due to incompressibility. In the present problem, where there is no hysteresis in the flow properties, the receding of the front is not an issue of concern. However, it is likely to be so in the case of immiscible displacements, where flow properties, for example relative permeabilities and capillary pressure, are indeed hysteretic²³. Upon breakthrough (Fig. 1d) both fronts arrive simultaneously at the sink.

To illustrate the advantage of the bang-bang control, we compared its displacement efficiency to the conventional case, where injection rates are constant. In particular, we considered the case, where the partition of the (constant) rates between the well is such that it maximizes the displacement efficiency. For most geometries, these rates are such that breakthrough in well C occurs simultaneously from both fronts (however, this not always true, as shown below). We will refer to this optimal case as constant-rate injection. Fig. 2 shows the fronts at breakthrough for the two different policies. The two displacements have different features. The swept area due to injection from well B in the constant rate case is much smaller than that for the bang-bang case. Because of its proximity to the sink, well B cannot accept a high injection rate, which will lead to early breakthrough. This is not so for the bang-bang case, where well B is put into action after some time has elapsed, thus it can accommodate a high (in fact, the highest) injection rate without the risk of a premature breakthrough. In the constant rate case, each source establishes its own “drainage” area, the shape of which is determined from the strength of the sources and the competition with other sources. The streamlines of the particles emanating from a given source, are thus restricted to this particular area, due to the flow fields from the other sources. In the bang-bang case, the fronts are not subject to this confinement. As shown previously, some of the streamlines emanating from the first well A will bend backwards, when injection from well B commences, and will eventually be diverted towards the sink C. This allows for a better displacement from well B and leads overall to a better displacement efficiency.

To assess quantitatively the effectiveness of the bang-bang policy, we compared the efficiency at breakthrough with that from the constant-rate injection. Fig. 3 shows a plot of the normalized breakthrough time as a function of the ratio of the distances between the two wells (always for a constant angle $\hat{A}CB = 45^\circ$). For all values of the latter, bang-bang injection gives a better displacement efficiency at breakthrough than the constant-rate case. The efficiency improvement depends on the distance ratio, with a maximum that in Fig. 3 can reach 13.7%, when the distance ratio is about 0.6. This improvement, although not very dramatic, is non trivial, given that it is accomplished only by flow rate control. Fig. 3 shows that the efficiency depends on the geometric arrangement of the wells, which essentially dictates the streamline lengths. We note that in heterogeneous fields, the efficiency

would additionally depend on the permeability structure, as possible spatial correlations will lead to channels and affect the streamlines (see Section II below). The switch time was found to decrease monotonically, from a value of 1 to a value of 0.342, as the distance ratio increased. It is worth noting, that for the constant-rate injection, optimal efficiency is not always associated with simultaneous injection from both wells. Thus, for a geometry with a distance ratio below approximately 0.6, injection from the closest injector (well B) does not improve the efficiency at breakthrough. Rather, the efficiency is maximized by injecting only from the farthest injector (well A, Fig. 3). Similar results were also found for other well arrangements and reservoir geometries¹⁶.

The bang-bang condition of the simultaneous arrival at the sink for optimal displacement efficiency can be interpreted readily. Indeed, consider a bang-bang policy, \mathcal{S} , in which when the front from well B first arrives in well C, the front from well A is at some finite distance away and during a finite time before breakthrough, injection occurs only from well B. We will show that \mathcal{S} is not the optimal injection policy. Indeed, given that the flow always remains potential, breakthrough of the front from well B will occur from particles moving along the diagonal BC, which is the fastest trajectory, when injection occurs only from well B, as assumed in this policy. Now, let us consider a time at a small time interval δt , before breakthrough, suitably chosen, and apply the different policy \mathcal{S}' , consisting of interrupting injection from well B and recommencing injection from well A in that time interval. It is clear that in this period of time, there will be no breakthrough of either front: Particles emanating from well B will now travel along curved, rather than straight streamlines, hence will not reach well C in time δt , while particles emanating from well A will not be sufficiently close to well C, under suitably small δt , in order to break through. Therefore, neither of these particles will reach breakthrough in this time interval, and policy \mathcal{S}' will lead to a higher displacement efficiency, contrary to our initial assertion. It follows that policy \mathcal{S} is not optimal. A similar argument holds if we were to reverse the roles of A and B, thus leading to the simultaneous arrival as a condition for an optimal bang-bang displacement.

From the above it can also be shown that the displacement efficiency of the bang-bang policy exceeds that of the two limiting cases, where only one of the two wells is active. Indeed, the bang-bang efficiency will be greater than that due to well B only, since by

construction the bang-bang policy includes, as a subset, injection until breakthrough from well B (this constitutes the second part of the policy, for example see Fig. 1). Proving that it is also greater than that from injection from well A only, follows by applying argument in the previous paragraph, in which the roles of wells A and B are reversed. In this sense, the efficiency of the bang-bang policy satisfies a “triangle inequality”.

4. Constraint on Injectivity

In the above, the overall rate was constrained to be constant. In certain practical cases, however, it is possible that the individual injection rates may not exceed a maximum value, which depends on the local conditions of the individual well. For example, we may have the constraint

$$0 \leq q_l(t) \leq q_{l,max} \quad ; \quad l = 2, \dots, N_W \quad (15)$$

where $q_{l,max}$ may not necessarily be the same for every l . Under this constraint, the optimal control formalism remains the same as before, except for the performance index, which now becomes

$$\mathcal{J} = \int_0^{t_f} \left(\sum_{l=2}^{N_W} q_l(t) \right) dt \quad (16)$$

Despite the different constraints, the linearity to the injection rates still remains, and the optimal injection policy is again predicted to be of the bang-bang type. The computational method for the solution of this problem is similar to the previous and details can be found in Sudaryanto¹⁶.

A number of numerical experiments were conducted for various constraints of the type (15) and for geometries similar to Fig. 1. In all cases, the optimal injection policy was found to have one switch time, as before. However, now there is the possibility that more than one injection wells are active simultaneously. Indeed, the optimal injection policy was found to consist of the following: (a) constant injection from the farthest injector and at its maximum rate throughout the process until breakthrough; and (b) no injection from the nearest injector until the switch time, after which injection commences at the maximum

injection rate for that well, until breakthrough. Here, the farthest injector was defined as the one which gives longer breakthrough times when injection is from that well only and at its maximum rate. Snapshots illustrating front movements for bang-bang injection under the injectivity constraints $0 \leq q_A \leq 0.5$ and $0 \leq q_B \leq 1$, are shown in Fig. 4. Commencement of injection at well B, after a certain time has elapsed (Fig. 4c), causes the streamlines from well A to bend towards well C, as in the case of Fig. 1. A comparison between the displacement efficiency at breakthrough between bang-bang and constant-rate injection policies is shown in Fig. 5. Here, because the overall rates are not constant, there is no equivalence between breakthrough times and displacement efficiency, however. The results show that bang-bang injection leads to both a better efficiency *and* a shorter breakthrough time, compared to constant-rate injection. Namely, here there is the additional benefit of faster recovery, associated with the bang-bang injection. The improvement in efficiency is similar to that for the constant overall rate constraint (Fig. 3). However, the reduction in breakthrough time can be significant and approaches 25%, in the best case, for the conditions of Fig. 5. This example shows that the injectivity constraints can play important and unexpected roles in the maximization of the displacement efficiency.

5. Experimental Results

To test the theoretical predictions, flow experiments in a Hele-Shaw cell were conducted. Although lacking the pore microstructure of actual porous media, Hele-Shaw cells are excellent experimental devices for the visualization of 2-D potential flows, under single-phase conditions. The Hele-Shaw cell consisted of two parallel 3/8 inch-thick glass plates of dimensions 24 inches x 18 inches separated by 1 inch-wide flat rubber strips placed along the edges of the cell that serve as a spacer (to maintain the gap thickness) and as a gasket (to seal the edges). The rubber strips have a thickness of 0.08 cm. Experiments were also conducted for a modified geometry, in which a large-scale flow barrier was added to the cell (see section II below). Three holes with a diameter of 1 cm were drilled in the bottom glass plate, two of which served as injection wells and the third as the production well. The injection wells were connected to two peristaltic (Masterflex) pumps, while the production well was connected to the ambient environment. The pumps were variable-flow computerized with easy-load pump

heads, and were connected to a PC, through which the variable flow rates were programmed and controlled according to the desired injection policy. In the experiments, dyed (methylene blue) water was injected to displace water originally in place, at a constant overall rate of 20 cc/min. A video camera mounted vertically above the cell captured the front movement. Injection policies corresponding to the optimal control policy as obtained above, as well as to constant rate injection were used. The schematic of the experimental set-up is shown in Fig. 6.

Snapshots of the displacement fronts under the optimal bang-bang policy are shown in Fig. 7. As discussed above, injection starts first from the more distant well, then switches at an optimal time to injection from the well nearest to the producer. Following the switch, the fluid originating from the more distant well is shown to be driven towards the production well, as expected theoretically. During this process, part of the front actually recedes, as predicted. The two fronts break through almost (but not exactly) at the same time. We believe that the reason for the slight discrepancy in front arrival is dispersion, which was not included in the theory. To estimate the effect of dispersion we used the standard Taylor-Aris expression for the dispersion coefficient

$$D = D_m + \frac{8u^2h^2}{945D_m} \quad (17)$$

where $2h = 0.08$ cm is the gap between the plates and $D_m \approx 10^{-5}$ cm²/sec is the molecular diffusivity. In rectilinear flows, the Peclet number is maximized at a specific value of the injection rate. Thus, operating at the smallest possible dispersion is possible by optimizing the overall injection rate. In our experiments, however, the displacement is not rectilinear, certainly not everywhere, and the Peclet number is spatially variable. To minimize dispersion, the experimental injection rate was chosen to be as close as possible to an optimal rate, subject, however, to the resolution constraints of the pumps, which did not allow for too small velocities. To provide a rough estimate of D the velocity was estimated as $u = 0.12$ cm/sec, away from the wells. This value will lead to the estimate $D \approx 0.02$ cm²/sec, which shows that dispersion cannot really be neglected (as it leads to spreading of the order of 1 inch for an experiment lasting for 300 seconds).

Fig. 8 shows snapshots of the displacement fronts at breakthrough from two different

flow experiments, one under the optimal bang-bang policy and another under constant-rate injection. For comparison, the results of the corresponding analytical approach, which is free of dispersion, are also shown. The two results are similar, but not identical. The area swept by the injected fluid at breakthrough in the physical experiments is slightly smaller and less compact compared to the corresponding area from the numerical experiments. We attribute this difference to the dispersion in the Hele-Shaw cell. Nonetheless, the efficiency was found to be higher under the optimal bang-bang policy than for the constant rate case. For the particular geometrical arrangement of Fig. 7, the ratio of the breakthrough time under bang-bang injection to that under constant-rate injection is predicted from the calculation to be 1.03. In fact, the result from the physical experiment is estimated to be slightly larger, 1.04, indicating that even in the presence of dispersion, the bang-bang policy is better than constant rate injection. (The relatively small improvement is here due to the particular geometrical arrangement considered. As shown in Fig. 3, the improvement in efficiency can reach larger values, depending on the geometry.) Additional experiments are discussed below in Section II.

II. Heterogeneous Porous Media

Consider, next, the optimization problem in a heterogeneous medium. It is well known that geological porous media exhibit a great degree of heterogeneity in permeability²⁴, the consideration of which is paramount for realistic predictions. Typically, the permeability is expressed in terms of a stochastic function in space, with various assumed forms of spatial correlation. A popular description is in terms of self-affine noise of the fBm type^{25–28} (fractional Brownian motion), where correlations grow with distance and the correlation length is unbounded. In such cases, the texture of the permeability field is characterized by its Hurst exponent H , $0 < H < 1$, larger values of H corresponding to a smoother field²⁶. For example, $H = 0.5$ corresponds to the classical Brownian motion. Examples of random and correlated permeability fields of this type are shown in Fig. 9. Layered reservoirs are also common. As in many applications involving geologic media, however, full knowledge of the heterogeneity structure is not available in the typical case. As a result, one has to

rely on a statistical description, in which a number of different permeability realizations are conducted, and from which results on average behavior can be extracted.

In this section, we will consider the optimal control problem for heterogeneous reservoirs in a miscible displacement with equal mobilities and in the absence of dispersion, as above. For simplicity, only the case with a constant overall injection rate constraint will be considered, other constraints being readily implemented. Now, as in the case of a homogeneous reservoir at unit mobility ratio, the state equations are linear with respect to the injection rates. Since the performance index to be maximized is also linear, then the non-singular optimal control is again of the bang-bang type.

However, in the heterogeneous case, we cannot take advantage of the potential flow formalism. Nonetheless, and because of the unit mobility ratio assumption, the displacement can still be expressed as a superposition of the response of individual wells. This facilitates considerably the problem description and its computation, as shown below. Unlike potential flow, where the well responses can be obtained analytically, however, displacements in heterogeneous reservoirs require a numerical solution.

1. Formulation

For simplicity, we will consider again a problem consisting of $N_W - 1$ injection wells of varying injection rates, and of one production well. Now, the flow field is obtained by solving the flow equations in a heterogeneous medium, namely we can write

$$\nabla \cdot k(\mathbf{x}) \nabla p = 0 \tag{18}$$

and

$$\mathbf{v}(\mathbf{x}, t) = -k(\mathbf{x}) \nabla p \tag{19}$$

with appropriate boundary conditions. Because the time dependence enters only through the boundary conditions, however, the velocity field can be also expressed in terms of the superposition of $N_W - 1$ two-well responses, namely

$$\mathbf{v}(\mathbf{x}, t) = \sum_{l=2}^{N_W} q_l(t) \mathbf{v}^{l,1}(\mathbf{x}) \quad (20)$$

where $\mathbf{v}^{l,1}(\mathbf{x})$ is the velocity field induced only by a two-well system, involving injection at unit strength in well l and production in well 1. Equation (20) shows that the variation in time is the superposition of the responses of individual well pairs, the spatial variation of which is independent of time and needs to be computed only once. This facilitates greatly the computation of the optimal control problem, which involves repeated iterations. Thus, the non-linear dynamical description derived for the homogeneous system remains valid, except that now the spatial dependence must be computed numerically, in general.

To proceed, we follow the same approach as in Section I, subject to the following changes. In equations, such as (3) for example, the sum must be rearranged to read

$$v_x = \sum_{l=2}^{N_W} q_l(t) \left[\frac{x - x_{wl}}{(x - x_{wl})^2 + (y - y_{wl})^2} - \frac{x - x_{w1}}{(x - x_{w1})^2 + (y - y_{w1})^2} \right] \quad (21)$$

Thus, the approach to be followed is identical, if the substitution is made

$$v_x^{l,1} \longleftrightarrow \sum_{l=2}^{N_W} q_l(t) \left[\frac{x - x_{wl}}{(x - x_{wl})^2 + (y - y_{wl})^2} - \frac{x - x_{w1}}{(x - x_{w1})^2 + (y - y_{w1})^2} \right] \quad (22)$$

In this way, the optimal control formalism becomes identical for the two problems. Calculation details can be found in Sudaryanto¹⁶. Here, we will briefly note the following: In the numerical solution, we used a block-centered finite-differences grid, the solution being computed at the center of each grid block. Harmonic averaging was used for the spatially varying permeabilities. The resulting matrix for the pressure was solved with an LSOR method. In tracking the front, expressions for the velocity coefficients in points other than the grid-block centers are often needed. These were obtained using multilinear interpolation from the values known at the four corner points of the square, within which the front resides at any given time. Likewise, the evolution of the Lagrange multipliers was obtained by solving numerically the corresponding equations, which now also involve evaluating numerically the spatial derivatives of $v_x^{l,1}$ and $v_y^{l,1}$ ($l = 2, \dots, N_W$). These were computed using three-point finite-differences. In some cases, streamtube simulation was also used. The optimal control computation was similar to Section I.

2. Numerical Results

Various forms of heterogeneity were used in the numerical experiments, including a large-scale flow barrier, a layered medium, and random and spatially correlated permeabilities of the fBm type.

In the first example, we considered a large-scale flow barrier intended to model the presence of an impermeable fault. The numerical results show that, in all cases, the optimal injection policy is bang-bang with one switch time. As before, the optimal switch time corresponds to the simultaneous arrival of the displacement fronts from the two injectors at the producer. Fig. 10 shows snapshots of the front movement under the optimal bang-bang injection policy. The particle tracking method used gives the expected results. The flow barrier impedes the flow towards the sink, while following the switch in injection, the front from well A is re-directed towards the sink. These results agree well with the results of flow experiments in the Hele-Shaw cell to be discussed below. Fig. 11 shows a comparison of the displacement efficiency at breakthrough under bang-bang and constant-rate injection policy. As expected, bang-bang injection outperforms constant-rate injection, with a maximum efficiency improvement of 13.8% in the particular geometry considered.

In the second example, we considered displacement in a layered reservoir, consisting of two regions with constant but different permeability values, k_1 and k_2 (e.g. see Fig. 12a, where $k_1 = 0.25k_2$). The numerical results show that, in most cases, the optimal injection policy has one switch time. However, for some geometries, two switch times are also possible. In all cases, the optimal policy involves steering the displacement fronts towards the low permeability region, first, to delay breakthrough as much as possible. Fig. 12 shows snapshots of the front movement under such a bang-bang policy, where two switch times are involved, corresponding right after the snapshots in Fig. 12b and 12c, respectively. The response of the streamlines after the switch in injection is apparent in the figure. As before, bang-bang injection gives better displacement efficiency at breakthrough than constant-rate injection for all distance ratio values tested¹⁶.

The last example of reservoir heterogeneity corresponds to random and spatially correlated fields. A log-normal permeability distribution with a modest permeability contrast of four ($k_{max} = 4k_{min}$) was studied. The uncorrelated field was generated by randomly assign-

ing values from a log-normal distribution. The spatially correlated fields were constructed using the successive random addition algorithm^{26,29}. In the numerical experiments, values of the Hurst exponent equal to 0.2, 0.5, and 0.8 were used. For each case, a total of 100 different realizations were generated. The results showed that the optimal injection policy is always bang-bang with one switch time. Snapshots of the front movement under the optimal bang-bang policy are shown in Fig. 13 for a particular realization of the uncorrelated case. An example of the correlated case is given in Fig. 14, where displacement fronts at breakthrough under bang-bang and constant-rate injection policy, and for a particular realization of the permeability field, are shown. The results show that bang-bang injection policy gives better displacement efficiency at breakthrough than constant-rate injection policy. Figures similar to Fig. 3 can be constructed for all these cases, but are not shown here for the sake of brevity. For example, for the particular realization of Fig. 13, the maximum efficiency improvement is in the range of 16%.

We must point out, that in addition to its dependence on well geometry, the improvement in efficiency depends on the particular realization of permeability field and the exponent H , however. Fig. 15 shows the efficiency improvement for a particular well geometry (a three-well system with distance ratio = 0.707 and angle $\alpha = 45^\circ$), for different realizations of the permeability field and different H exponents. The range of efficiency improvement is essentially the same for each model of spatial correlation, almost independent of the value of the Hurst exponent. However, the efficiency improvement varies significantly from one realization to another, reflecting the different spatial arrangement of the flow paths. Another illustration of this effect is the variation of the (normalized) switch time of the bang-bang policy (Fig. 16). This time is shown to vary in a relatively narrow range (from about 0.85 to 1.05) for the case of uncorrelated permeability fields. As the spatial correlation increases, however, the range of variation increases significantly (from about 0.7 to 1.3) and it has a weak increasing dependence on H .

3. A Sensitivity Study

To complete the study of heterogeneity, we considered a sensitivity study, in which we posed the question what would be the reduction in efficiency, if the heterogeneity of the

medium were ignored in the designing of the displacement process. To address this question, we compared the displacement efficiency at breakthrough from the application of a bang-bang injection policy, which is optimal for the assumed homogeneous problem, to that from constant-rate injection policy which is also optimal for the same assumed homogeneous reservoir. Answering this question will essentially dictate whether the advantage of bang-bang over constant rate optimal injection carries over to heterogeneous systems, even though they were both designed on the assumption that the reservoir is homogeneous. Numerical experiments were conducted for one particular well geometry, namely a three-well system with distance ratio = 0.707 and an angle of 45° . The permeability of the homogeneous medium was taken equal to the mean value of the heterogeneous field. For the heterogeneous problem we considered the previous (modestly heterogeneous) models.

The results are shown in Fig. 17. In almost all cases (the two exceptions in the random case are probably due to numerical error), bang-bang injection gives a better displacement efficiency at breakthrough than constant-rate, even though it was designed on the assumption of a homogeneous reservoir. On average, the improvement and its variance increase as the spatial correlation of the permeability becomes stronger. Thus, the benefits of bang-bang injection carry over (even more accentuated) to the heterogeneous case. In assessing these results one should also note that the permeability contrast was taken to be relatively narrow (only a factor of 4). In many realistic situations, permeability contrasts of much larger magnitude, reaching several orders of magnitude, are not uncommon. Under such conditions, we expect that optimal bang-bang policies will offer additional quantitative improvement.

4. Experiments

Experiments corresponding to the geometry of the first example in the previous subsection were also carried out. We used the previous Hele-Shaw cell with a large-scale flow barrier (Fig. 18), put in place using a 4 inch x 1 inch rubber strip between the glass plates. Shown in Fig. 18 are snapshots of the front movement under the optimal bang-bang injection policy computed as described above. The corresponding numerical results were given in Fig. 10 and show very similar features. By appropriately switching the injection rates, both fronts are steered towards the production well, in which they arrive at almost the same time as

predicted (the slight discrepancy due again to dispersion). The difference with the constant injection rate case (where the rates were chosen to optimize the displacement efficiency) is shown in Fig. 19. The final configurations are different, with more displacement due to injection from the nearest well, in the bang-bang case. The improvement in the efficiency ratio between bang-bang and constant rate policies was estimated to be 1.06 in the physical flow experiments, compared to a predicted value of 1.05. As with the previous case, this slight difference is probably due to the presence of dispersion in the physical experiment.

Conclusions

In this paper, the problem of the control of flows, and more specifically of displacement fronts, in porous media by controlling the injection rates at various point sources, was addressed. We presented an approach based on optimal control theory to maximize the displacement efficiency at breakthrough in 2-D miscible displacements, when the mobilities of the two fluids are the same, and effects of gravity and dispersion are negligible. The approach relies on formulating the problem as a non-linear dynamics problem for the particles that define the front. In the case of homogeneous media, this formulation is analytic. In the case of heterogeneous media, we used a superposition approach to separate time and spatial dependences, which substantially reduces the computational requirements.

It was found that the non-singular optimal control policy is of the bang-bang type, namely a policy in which any given well operates at any time at the extreme limits of its injection rate. Then, the problem becomes one of determining the optimal switch times for each well. Depending on the problem, multiple switch times are possible, although most examples shown correspond to one switch time only. Numerical results showed that this policy leads to an improved displacement efficiency at breakthrough, compared to the case of constant rate injection. The improvement is based on the underlying assumption that miscible flows are not direction-dependent, hence displacement fronts emanating from a given source, can recede and change direction reversibly, upon the activation of another source. This assumption may not hold for immiscible flows where flow properties are hysteretic. Sensitivity studies in heterogeneous media showed that the results depend sensitively on the particular realization of the permeability field, as well as on the presence or absence of spatial

correlation. In particular, it was shown that on average, the advantages of the bang-bang control remain, and in fact become greater, compared to constant-rate injection, even if one were to design the optimal control process in the absence of information on the permeability heterogeneity. Experimental results in a Hele-Shaw cell supported to a certain extent, the theoretical findings.

The above theory can be extended to address problems of variable mobility and of immiscible displacements¹⁴. Objective functions other than the displacement efficiency at breakthrough of the injected fluid, considered here, are amenable to a similar analysis. Likewise, extensions to more complex problems, particularly in 3-D with partially active sources, etc., are feasible. These problems capture important temporal and spatial dynamical features of flows in porous media as a result of the time dependence of injection rates at various point sources. In particular, they are related to the more general problem of the dynamics of deformation of material lines in porous media flows, which is a subject of further research¹⁶.

Acknowledgements

This research was partly supported by DOE Contract DE-FG22-96BC1994/SUB and by PERTAMINA, the contributions of which are gratefully acknowledged.

¹M. Muskat, *The Flow of Homogeneous Fluids through Porous Media*, McGraw-Hill, New York (1937).

²J. Bear, *Dynamics of Fluids in Porous Media*, Dover, New York (1988).

³W.F. Ramirez, Z. Fathi, and J.L. Cagnol, "Optimal injection policies for enhanced oil recovery : Part 1- Theory and computational strategies," SPE Journal, 328 (1984).

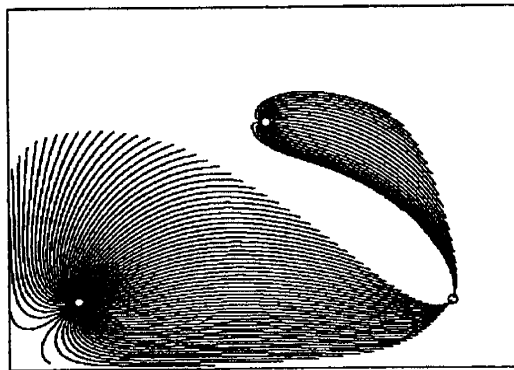
⁴Z. Fathi and W.F. Ramirez, "Optimal injection policies for enhanced oil recovery : Part 2- Surfactant flooding," SPE Journal, 333 (1984).

⁵Z. Fathi and W.F. Ramirez, "Use of optimal control theory for computing optimal injection policies for enhanced oil recovery," *Automatica* **22** (1), 333 (1986).

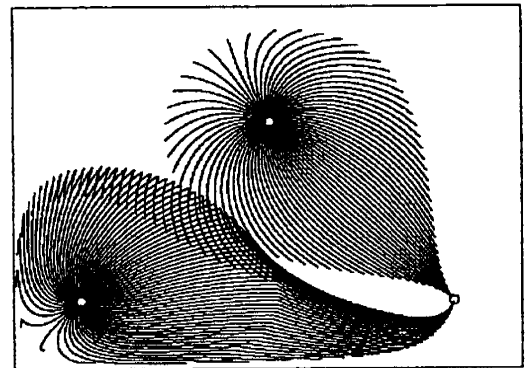
⁶Z. Fathi and W.F. Ramirez, "Optimization of an enhanced oil recovery process with boundary controls: a large-scale non-linear maximization," *Automatica* **23** (3), 301 (1987).

- ⁷W.F. Ramirez, *Application of Optimal Control Theory to Enhanced Oil Recovery*, Elsevier, Amsterdam (1987).
- ⁸H. Asheim, "Maximization of water sweep efficiency by controlling production and injection rates," paper SPE 18365 presented at the SPE European Petroleum Conference, London, UK, Oct. 16-19, 1988.
- ⁹G.A. Virnovsky, "Waterflooding strategy design using optimal control theory," paper presented at the 6th European IOR Symposium, Stavanger, Norway, May 21-23, 1991.
- ¹⁰S.B. Gorell and G.M. Homsy, "A theory of the optimal policy of oil recovery by secondary displacement processes," *SIAM J. Appl. Math.* **43**, 79 (1983).
- ¹¹G.M. Homsy, "Viscous fingering in porous media," *Annu. Rev. Fluid Mech.* **19**, 271 (1987).
- ¹²Y.C. Yortsos, "Instabilities in displacement processes in porous media," *J. Phys.: Condens. Matter* **2**, SA 443 (1990).
- ¹³P. Petitjeans, C.-Y. Chen, E. Meiburg and T. Maxworthy, "Miscible quarter five-spot displacements in a Hele-Shaw cell and the role of flow-induced dispersion," *Phys. Fluids* **11**, 1705 (1999).
- ¹⁴B. Sudaryanto and Y.C. Yortsos, "Optimization of Fluid Front Dynamics in Porous Media Using Rate Control: II. Variable Mobility Fluids," to be submitted.
- ¹⁵J.M. Ottino, *The Kinematics of Mixing: Stretching, Chaos and Transport*, Cambridge University Press, Cambridge (1989).
- ¹⁶B. Sudaryanto, "Optimization of displacement efficiency of oil recovery in porous media using optimal control theory," Ph.D. Dissertation, University of Southern California (1998).
- ¹⁷N.V. Dokholyan, Y. Lee, S. Buldyrev, S. Havlin, P.R. King and H.E. Stanley, "Scaling of the distribution of shortest paths in percolation," *J. Stat. Phys.* **93**, 603 (1998).
- ¹⁸A.E. Bryson, Jr. and Y.C. Ho, *Applied Optimal Control: Optimization, Estimation, and Control*, Hemisphere, Washington, DC. (1975).
- ¹⁹K. Gashoff and E. Sachs, "On theoretical and numerical aspects of the bang-bang principle," *Numer. Math.* **29**, 93 (1977).
- ²⁰R.R. Mohler, *Nonlinear Systems, Volume II: Applications to Bilinear Control*, Prentice Hall, Englewood Cliffs, NJ (1991).

- ²¹C.Y. Kaya and J.L. Noakes, "Computations and time-optimal controls," *Optimal Control Appl. Meth.* **17**, 171 (1996).
- ²²E.B. Meier and A.E. Bryson, Jr., "Efficient algorithm for time-optimal control of a two-link manipulator", *J. Guid. Control Dyn.* **13**, 85 (1990).
- ²³F.A.L. Dullien, *Porous Media: Fluid Transport and Pore Structure*, Academic Press, New York (1992).
- ²⁴G. Dagan, *Flow and Transport in Porous Formations*, Springer-Verlag, Berlin (1989).
- ²⁵T.A. Hewett, "Fractal distributions of reservoir heterogeneity and their influence on fluid transport", paper SPE 15386 presented at 61st Annual Technical Conference and Exhibition of SPE, New Orleans, LA Oct. 5-8, 1986.
- ²⁶J. Feder, *Fractals*, Plenum Press, New York (1988).
- ²⁷A.-L. Barabasi and H.E. Stanley, *Fractal Concepts in Surface Growth*, Cambridge University Press, Cambridge (1995).
- ²⁸C. Du, C. Satik and Y.C. Yortsos, "Percolation in a fractional Brownian motion lattice," *AICHEJ* **42**, 2392 (1996).
- ²⁹H.O. Peitgen and D. Saupe, *The Science of Fractal Images*, Springer-Verlag, New York (1988).



(a) Constant-rate injection policy



(b) Bang-bang injection policy

Figure 1: Snapshots of front movement under bang-bang injection policy. (a) At initial time, (b) at time just before the injection switches from well A to well B, (c) at time when injection is only through well B. [Note the bending of the trajectories following the switch of injection from well-A to well-B], and (d) at breakthrough. (Potential flow, rectangular reservoir, distance ratio equal to 0.7, angle equal to 45° .)

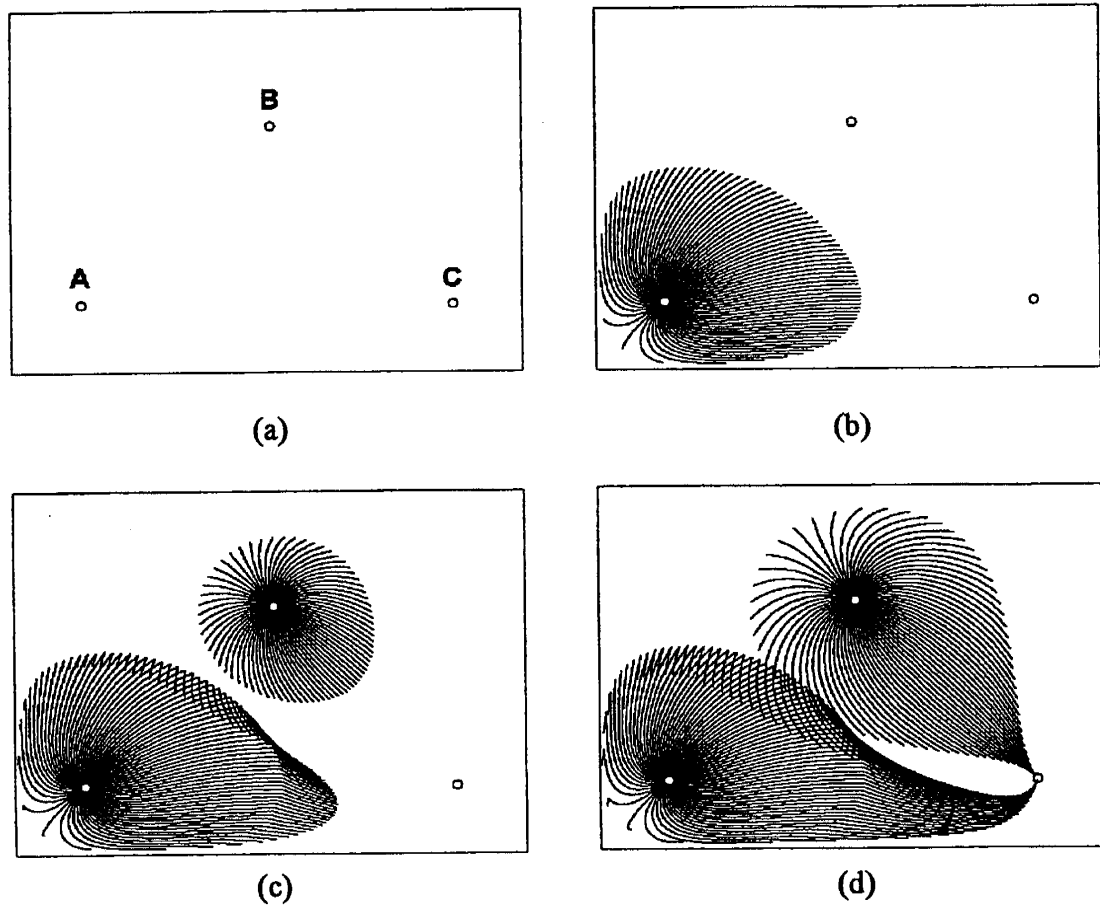


Figure 2: Displacement fronts at breakthrough under constant-rate and bang-bang injection policies. (Potential flow, rectangular reservoir, distance ratio equal to 0.7, angle equal to 45° .)

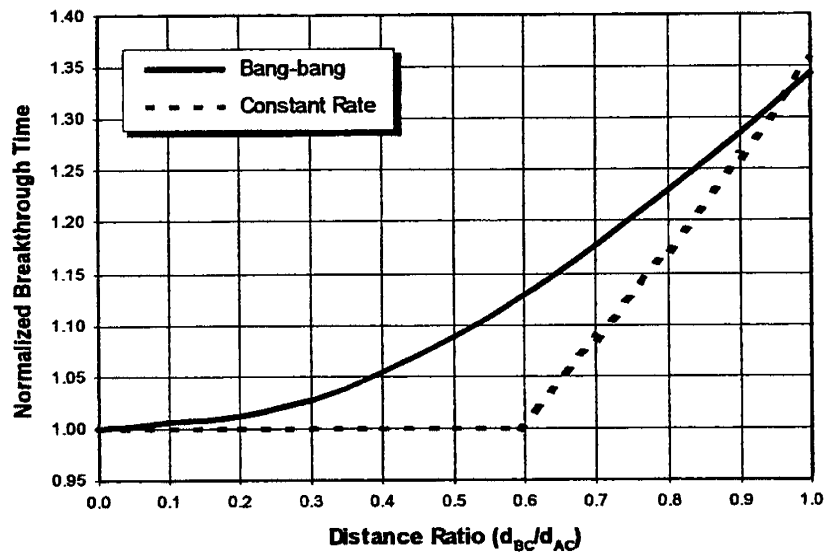


Figure 3: Normalized breakthrough time under constant-rate and bang-bang injection policies as a function of the distance ratio. (Potential flow, rectangular reservoir, distance ratio equal to 0.7, angle equal to 45°.)

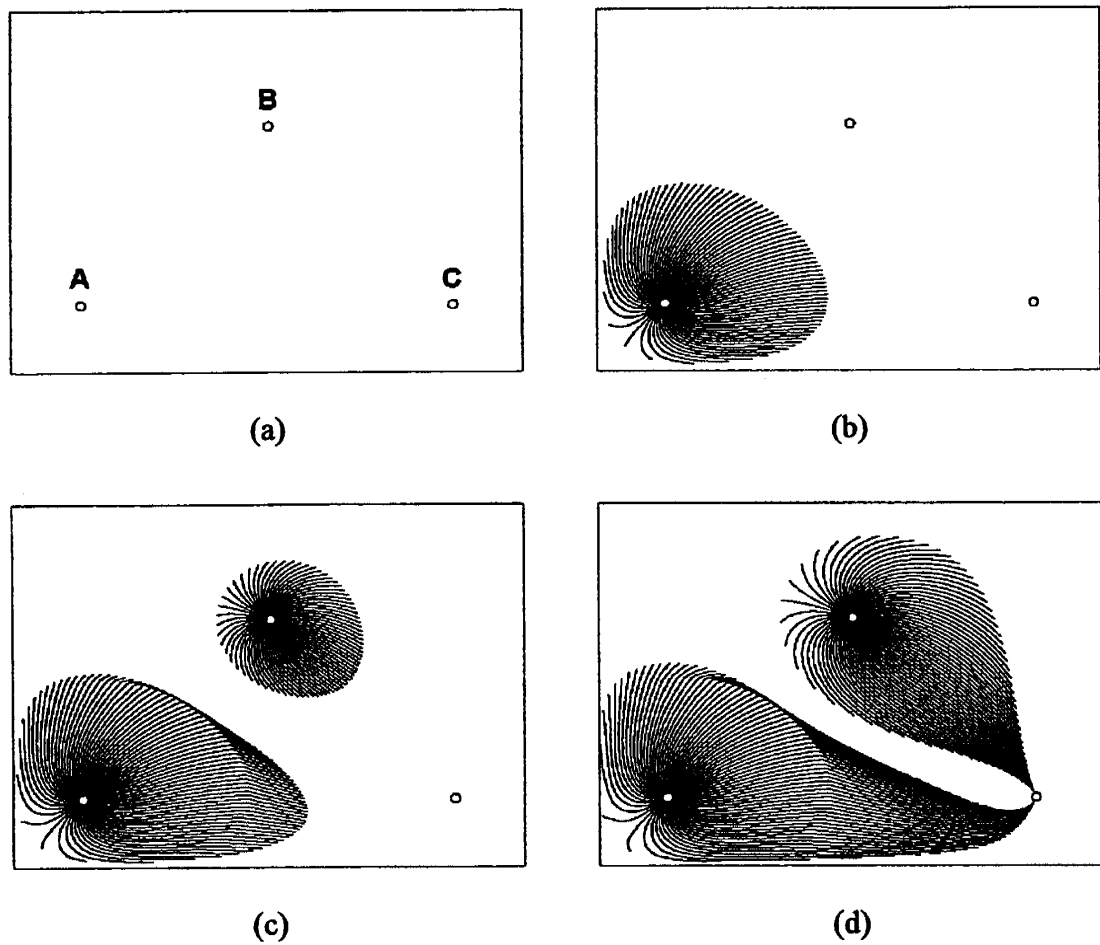


Figure 4: Snapshots of front movement under bang-bang injection policy. (a) At initial time, (b) at time just before injection from well B started, (c) at time when both injectors A and B are active, and (d) at breakthrough. (Potential flow, rectangular reservoir, distance ratio equal to 0.7, angle equal to 45° , well injectivity constraint.)

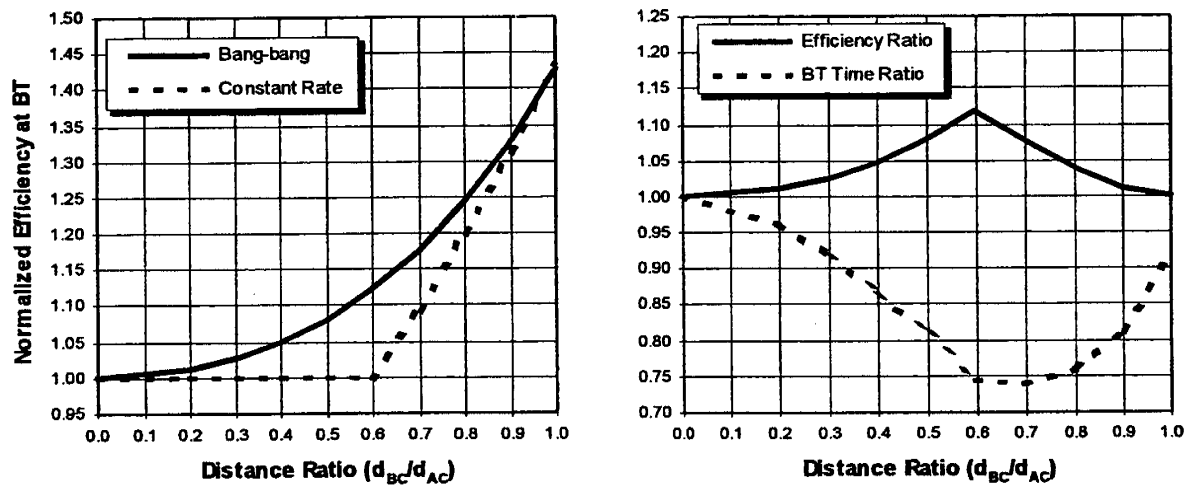


Figure 5: Efficiency at breakthrough (left), efficiency ratio and breakthrough time ratio (right) as a function of the distance ratio. (Potential flow, rectangular reservoir, angle equal to 45° , well injectivity constraint.)

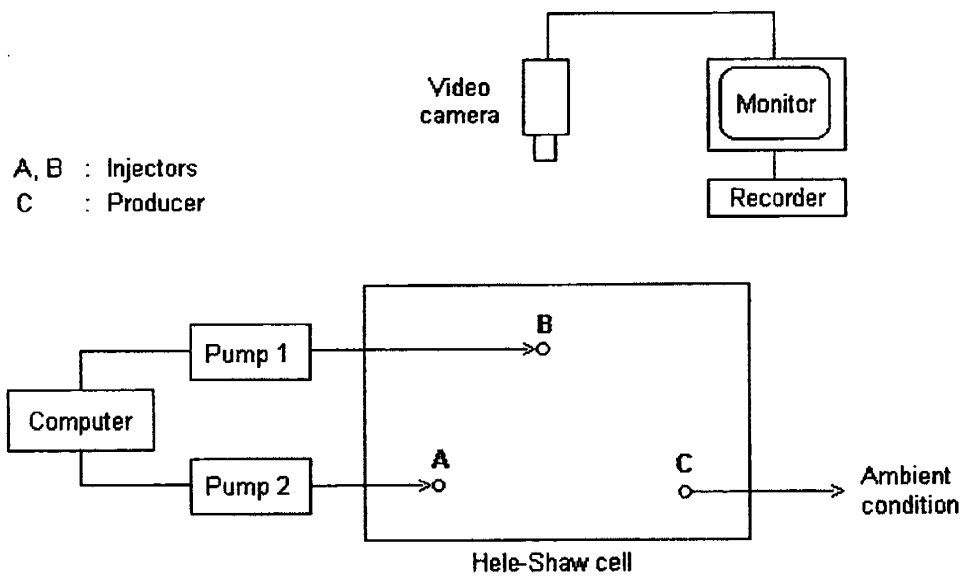


Figure 6: Schematic of the experimental set-up.

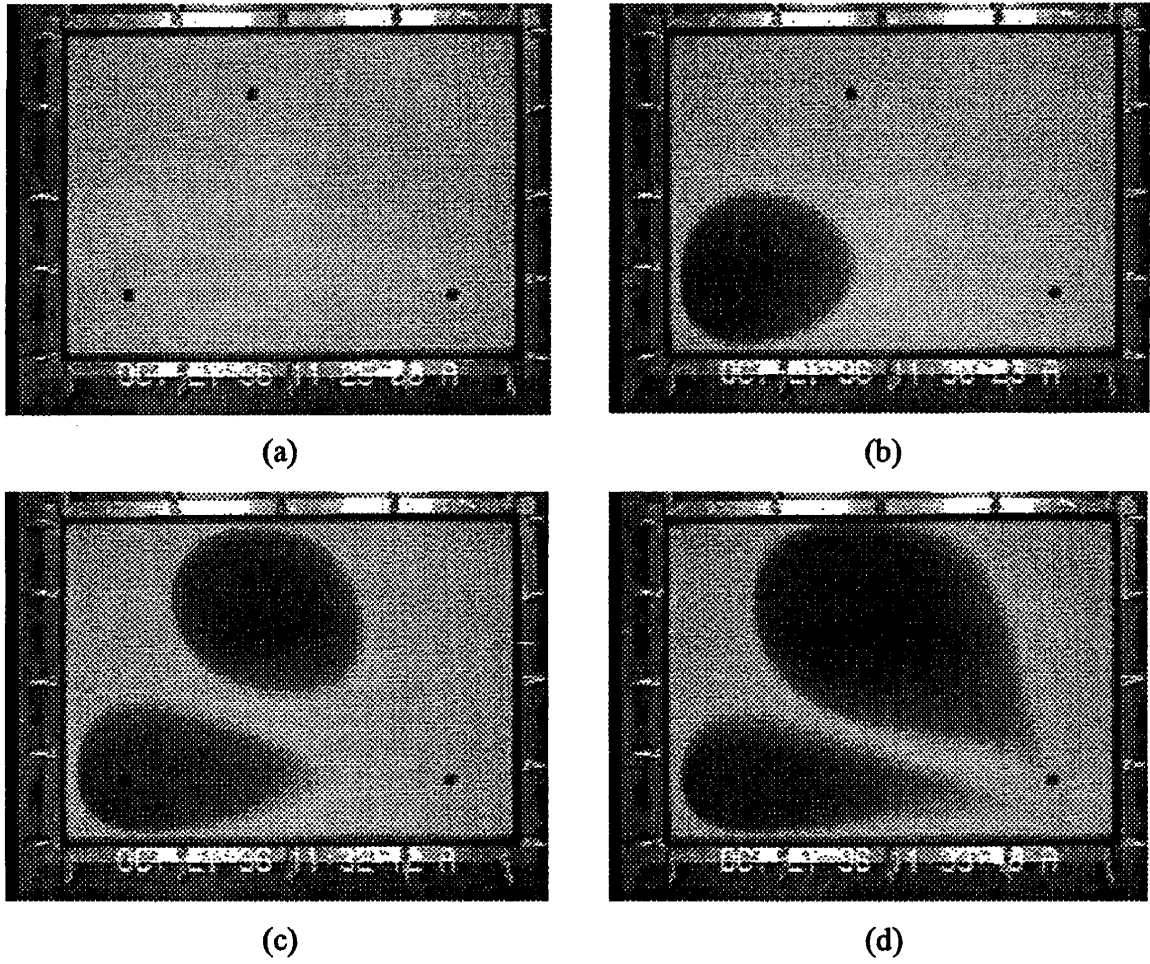
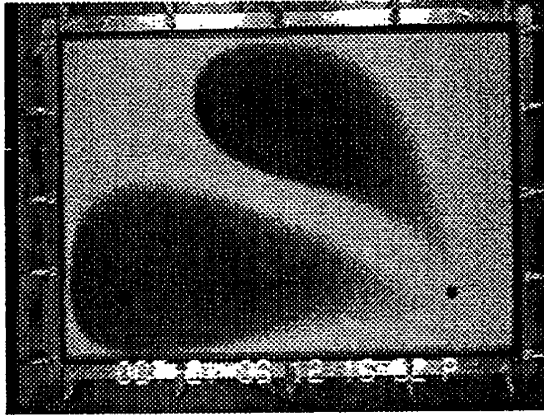
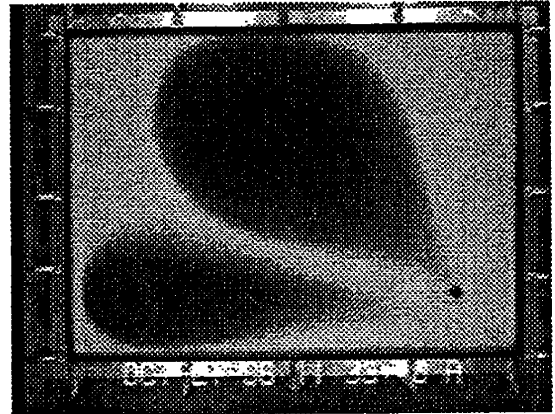


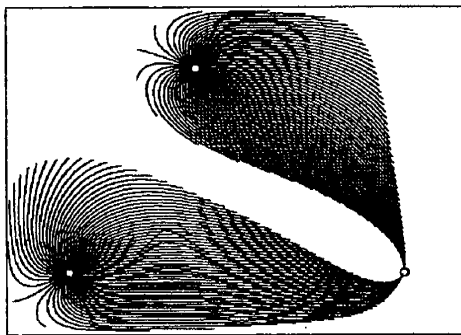
Figure 7: Experimental snapshots of front movement under bang-bang injection policy. (a) At initial time, (b) at time just before the injection switches from well A to well B, (c) at time when injection is only through well B, and (d) at breakthrough. (Tracer displacement in a rectangular Hele-Shaw cell, distance ratio equal to 0.884, angle equal to 45° .)



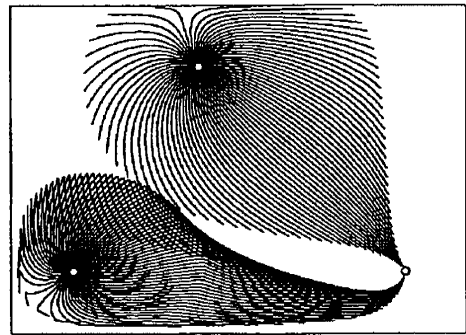
(a) Constant-rate injection policy



(b) Bang-bang injection policy

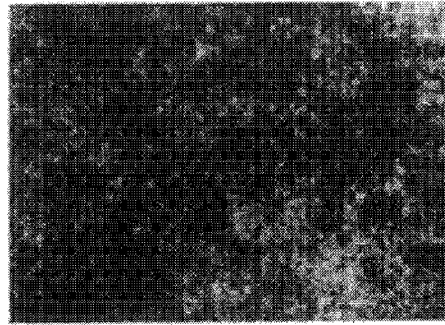


(a) Constant-rate injection policy

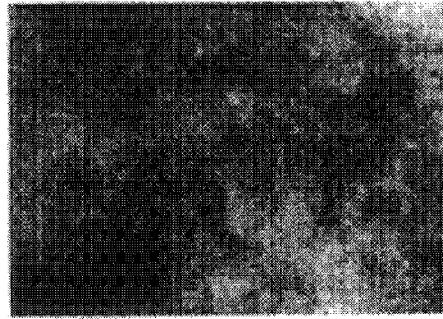


(b) Bang-bang injection policy

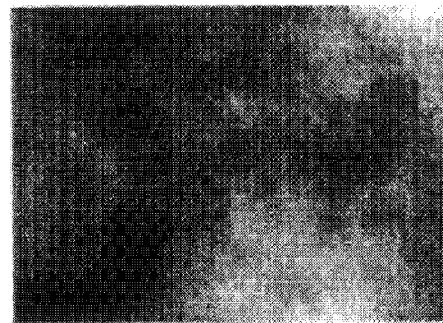
Figure 8: Comparison between experimental (top) and numerical results (bottom) for the displacement patterns at breakthrough under constant-rate (left) and bang-bang (right) injection.



(a)



(b)



(c)

Figure 9: Realizations of correlated permeability fields of the fBm type with Hurst exponents $H=0.2$, 0.5 and 0.8 .

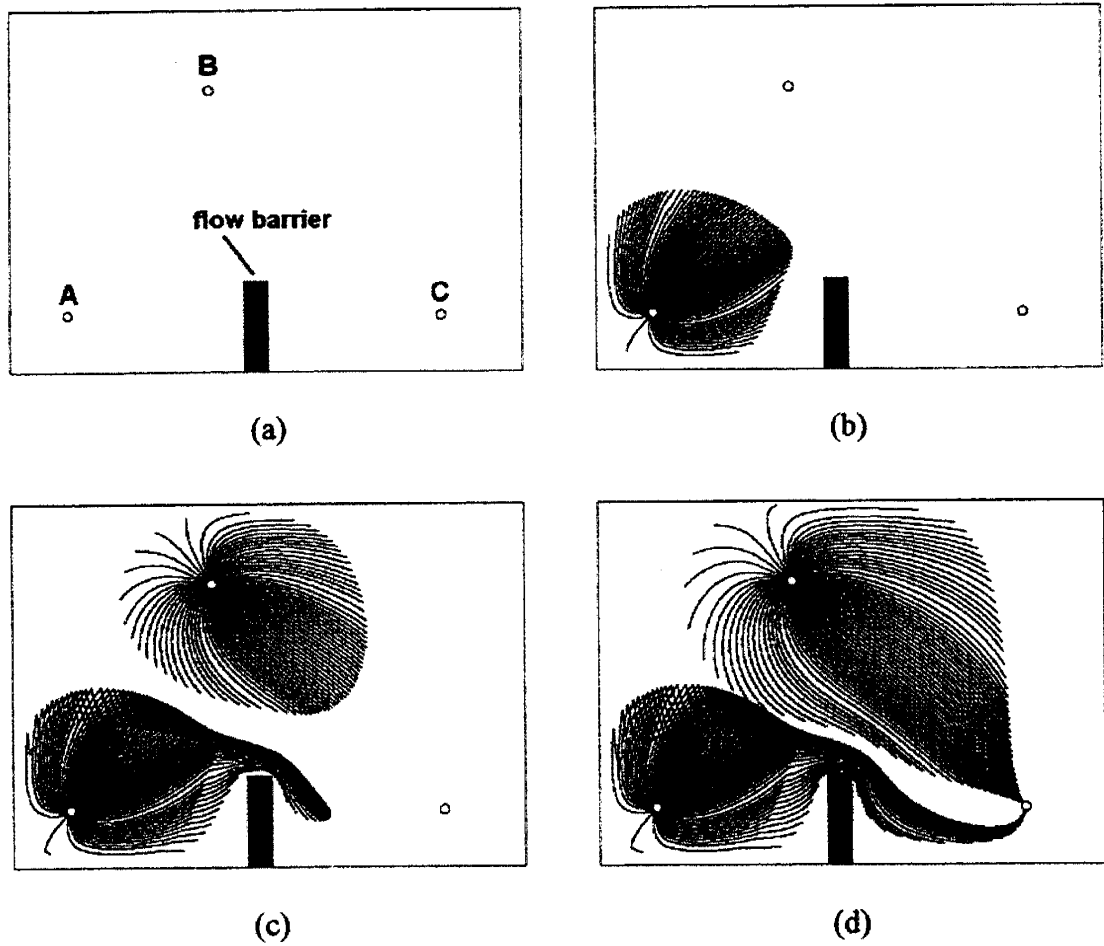


Figure 10: Snapshots of front movement under bang-bang injection policy. (a) At initial time, (b) at time just before injection switches to well B, (c) at time when injection is only through well B, and (d) at breakthrough. (Potential flow, rectangular reservoir with a flow barrier, distance ratio equal to 0.884, angle equal to 45° .)

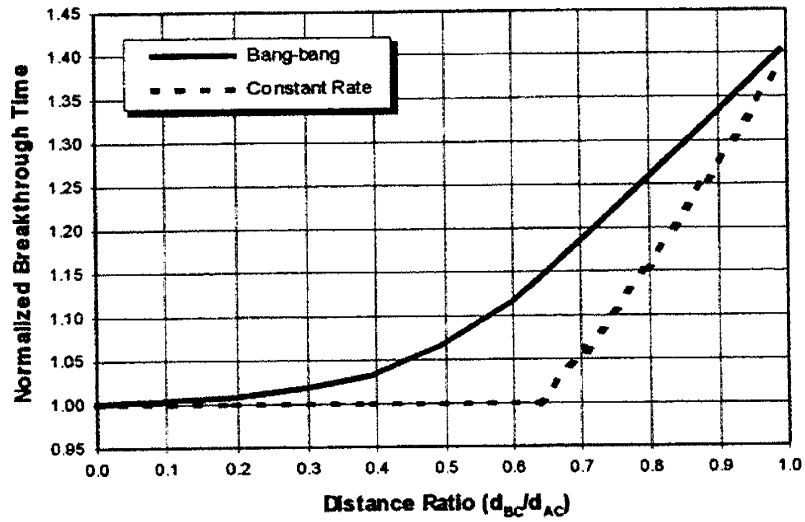


Figure 11: Normalized breakthrough time under constant-rate and bang-bang injection policy as a function of the distance ratio. (Potential flow, rectangular reservoir with a flow barrier, distance ratio equal to 0.884, angle equal to 45° .)

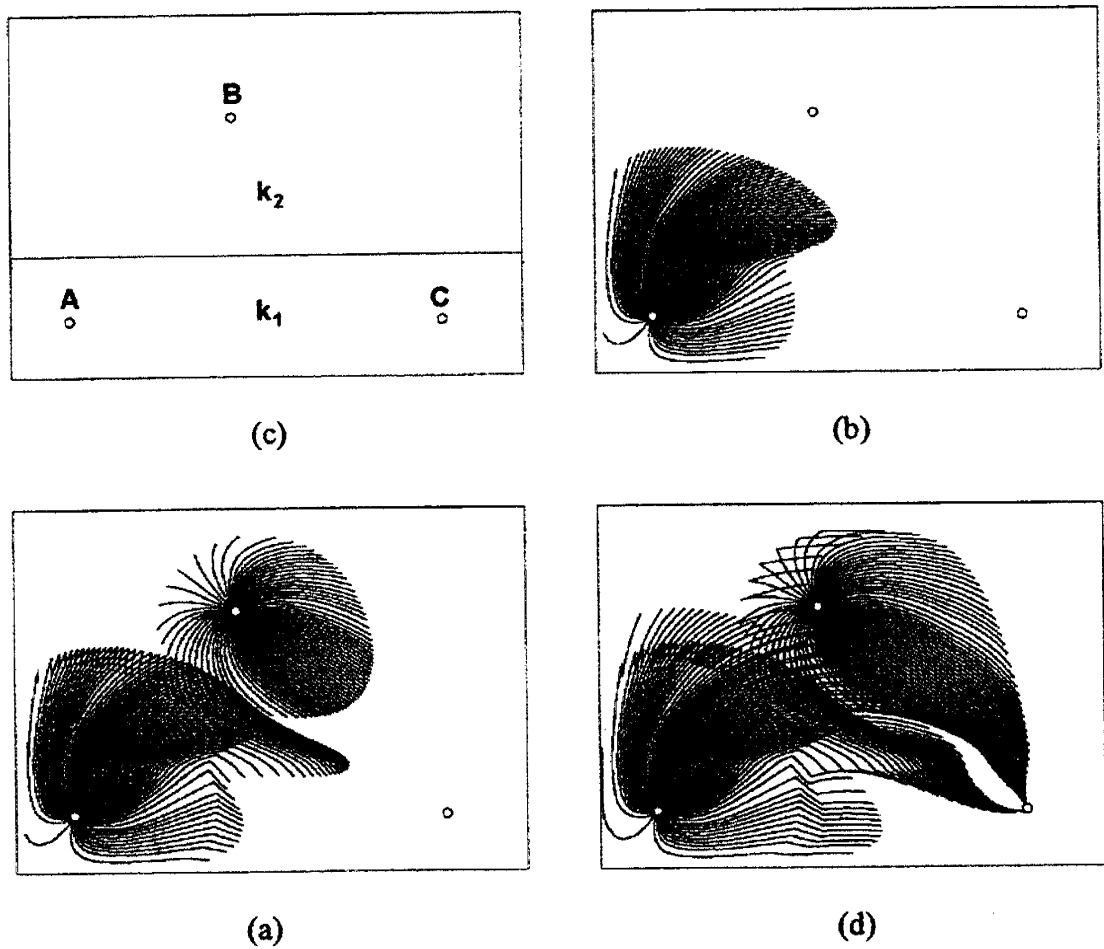


Figure 12: Snapshots of front movement under bang-bang injection policy. Two switch times are involved: (a) At initial time, (b) at time just before injection switches to well B, (c) at time just before injection switches back from well B to well A, and (d) at breakthrough. (Layered reservoir, $k_1 = 0.25 k_2$, distance ratio equal to 0.795, angle equal to 45° .)

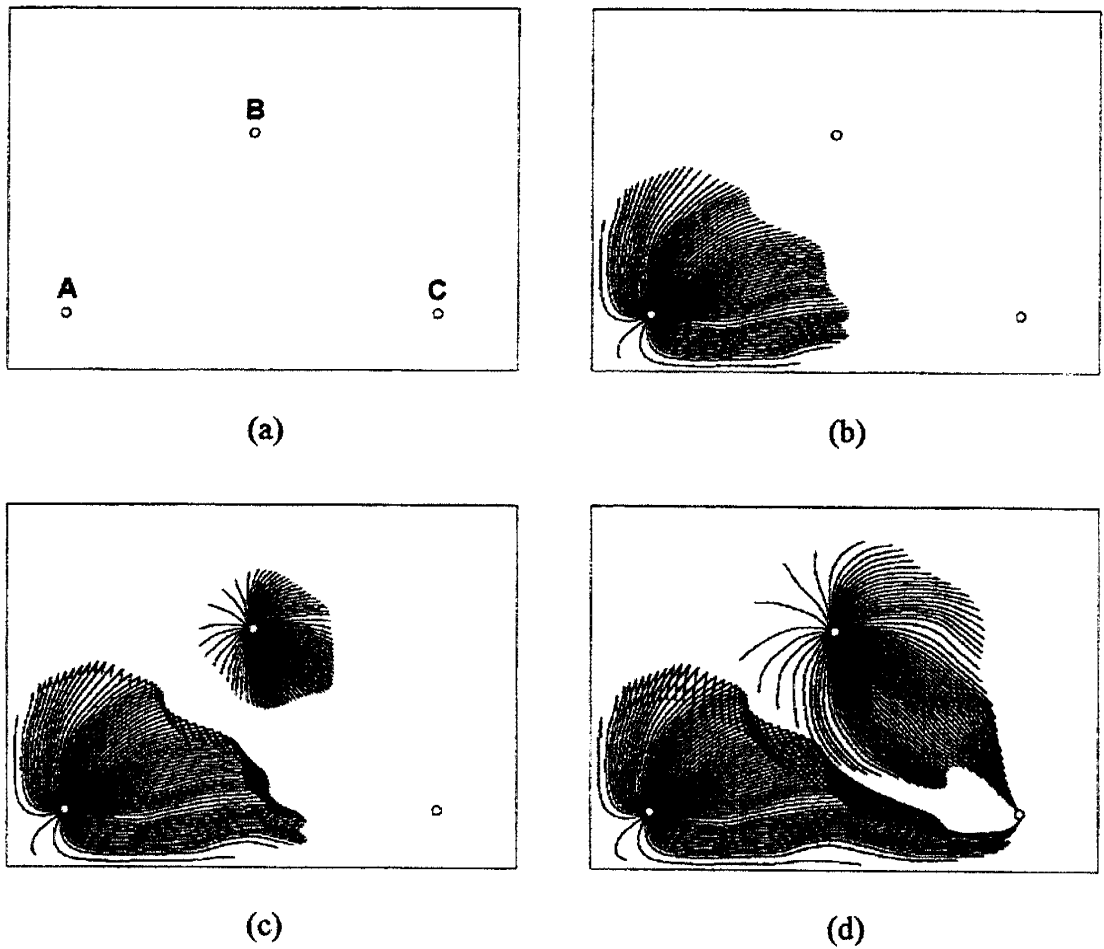
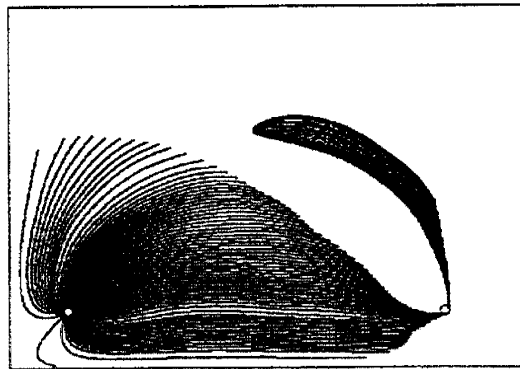
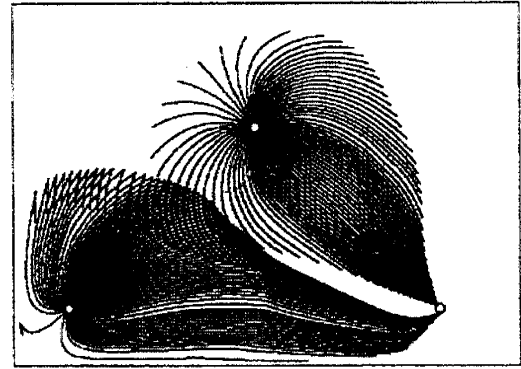


Figure 13: Snapshots of front movement under bang-bang injection policy. Two switch times are involved: (a) At initial time, (b) at time just before injection switches to well B, (c) at time when injection is only through well B, and (d) at breakthrough. (Random permeability field, distance ratio equal to 0.707, angle equal to 45° .)

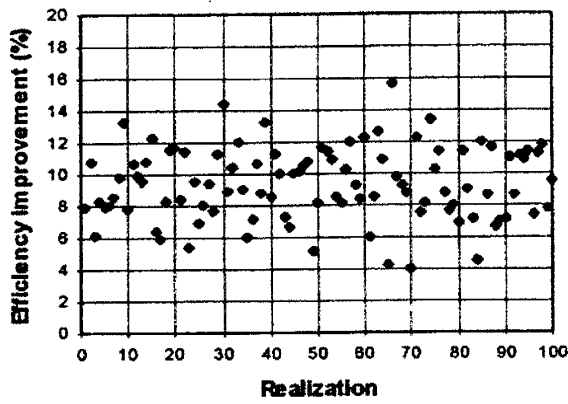


(a) Constant-rate injection policy

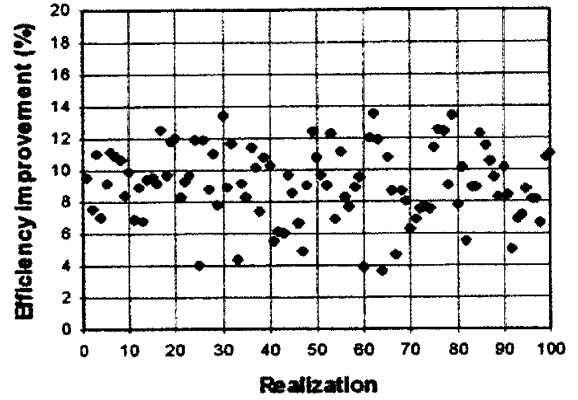


(b) Bang-bang injection policy

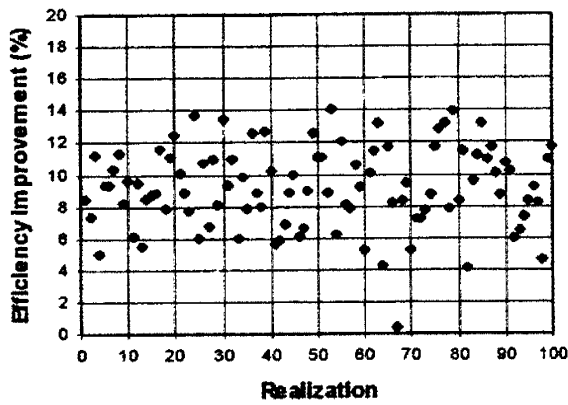
Figure 14: Displacement fronts at breakthrough under constant-rate and bang-bang injection policies. (Correlated (fBm) permeability field with $H=0.8$, distance ratio equal to 0.707, angle equal to 45° .)



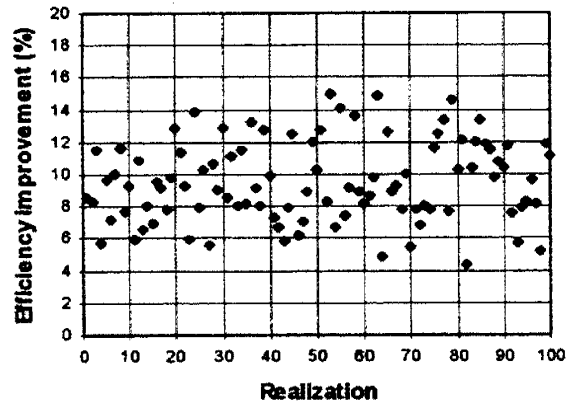
[a] Uncorrelated (random)



[b] Correlated (fBm, $H=0.2$)

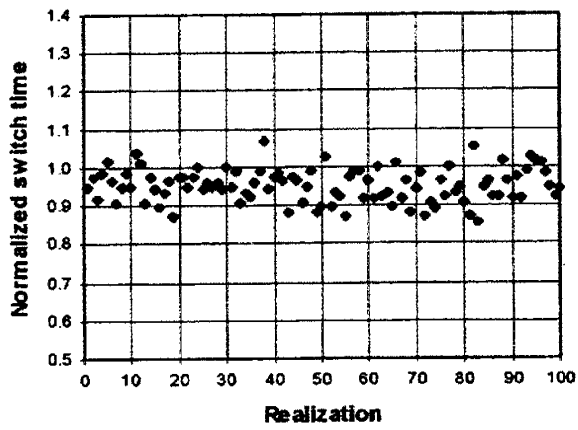


[c] Correlated (fBm, $H=0.5$)

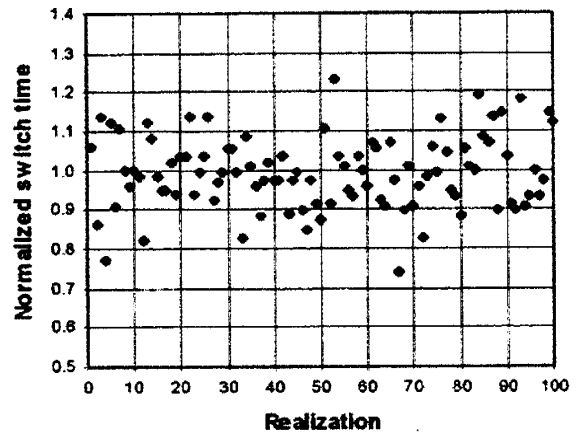


[d] Correlated (fBm, $H=0.8$)

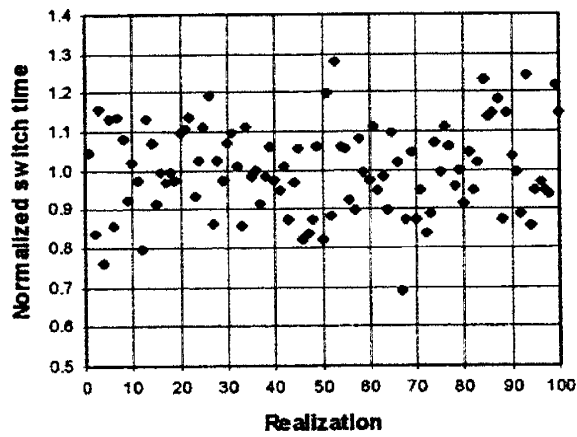
Figure 15: Efficiency improvement of bang-bang over constant-rate injection policy for different realizations of uncorrelated and correlated permeability fields.



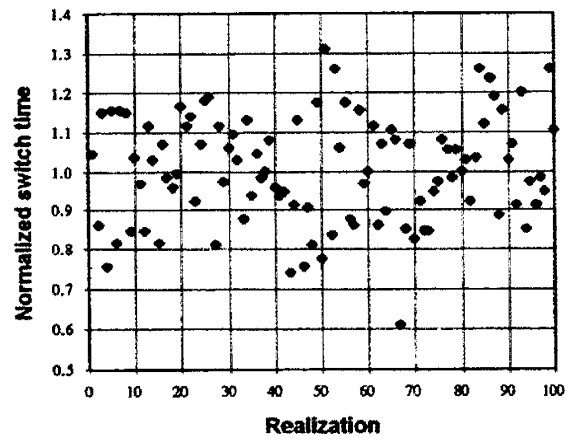
[a] Uncorrelated (random)



[b] Correlated (fBm, $H=0.2$)

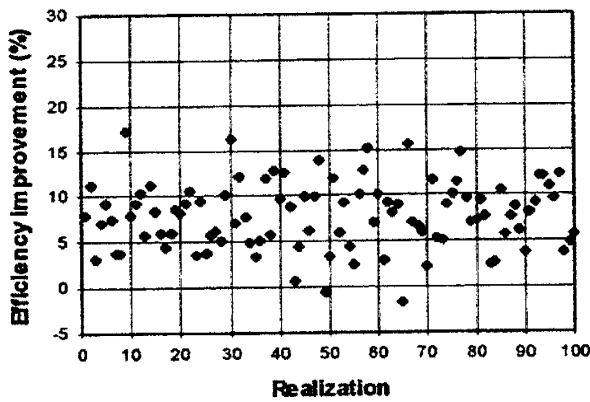


[c] Correlated (fBm, $H=0.5$)

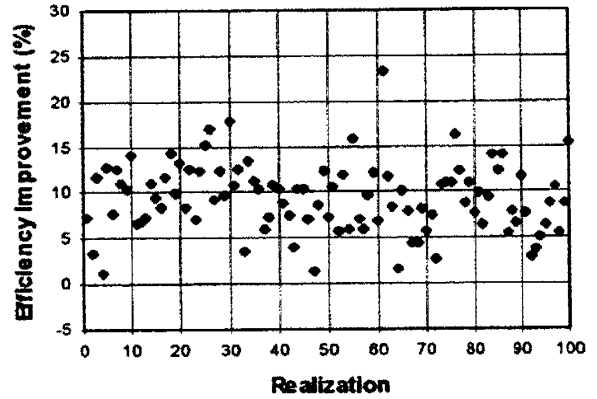


[d] Correlated (fBm, $H=0.8$)

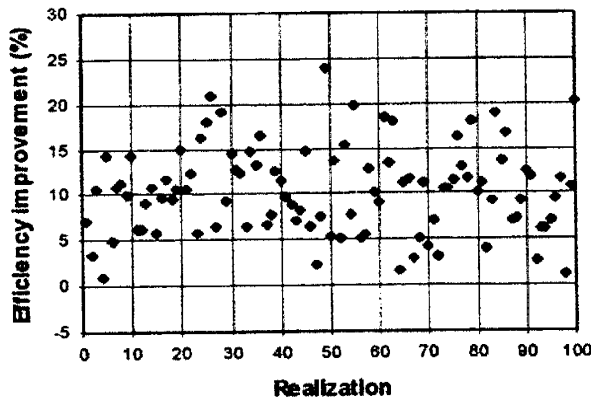
Figure 16: Normalized optimal switch time for different realizations of uncorrelated and correlated permeability fields.



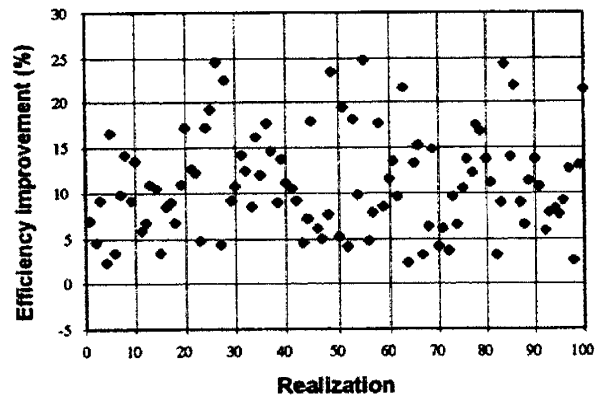
[a] Uncorrelated (random)



[b] Correlated (fBm, $H=0.2$)



[c] Correlated (fBm, $H=0.5$)



[d] Correlated (fBm, $H=0.8$)

Figure 17: Efficiency improvement of bang-bang over constant-rate injection policy (both injection policies are optimal for a homogeneous system) for different realizations of uncorrelated and correlated permeability fields.

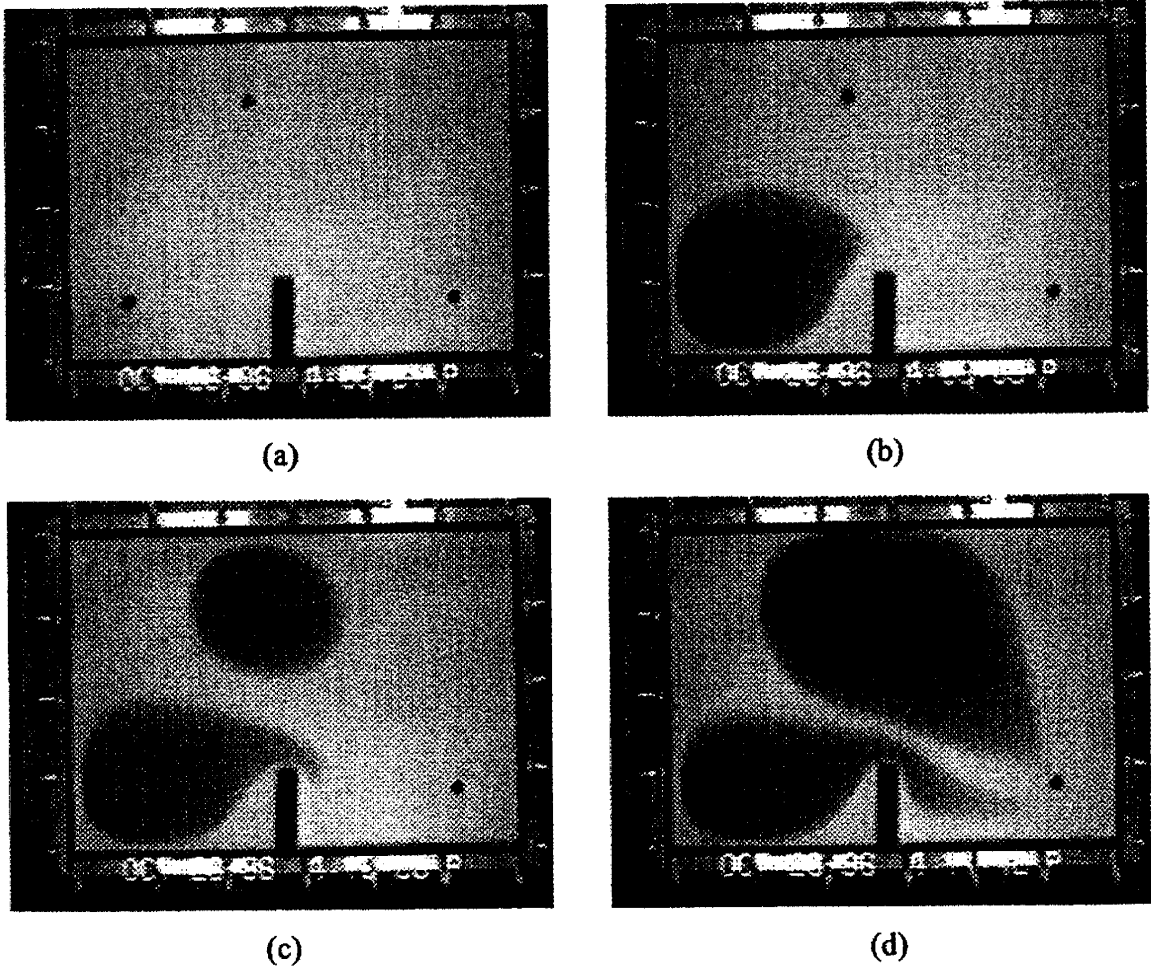
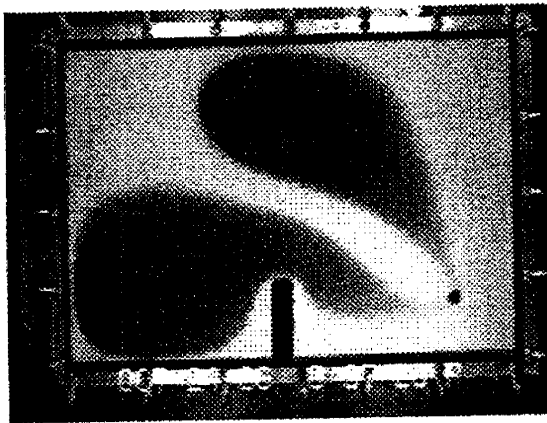
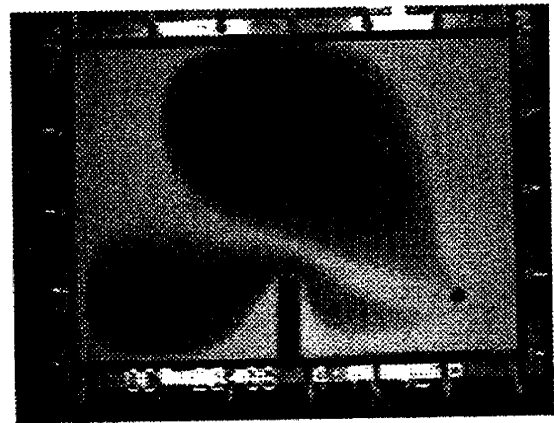


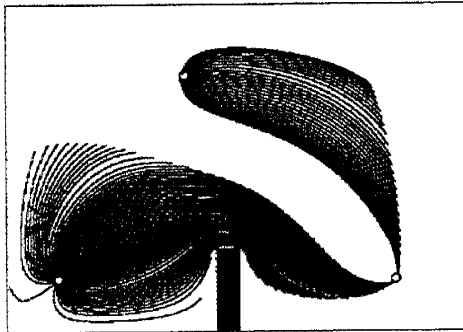
Figure 18: Experimental snapshots of front movement under bang-bang injection policy. (a) At initial time, (b) at time just before the injection switches from well A to well B, (c) at time when injection is only through well B, and (d) at breakthrough. (Tracer displacement in a rectangular Hele-Shaw cell with a flow barrier, distance ratio equal to 0.884, angle equal to 45° .)



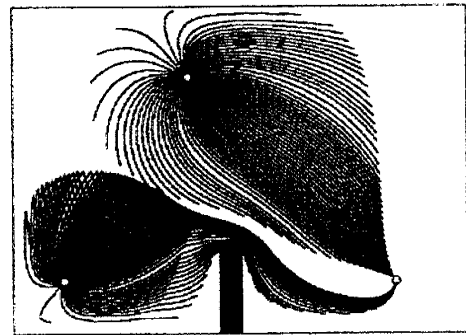
(a) Constant-rate injection policy



(b) Bang-bang injection policy



(a) Constant-rate injection policy



(b) Bang-bang injection policy

Figure 19: Comparison between experimental (top) and numerical results (bottom) for the displacement patterns at breakthrough under constant-rate (left) and bang-bang (right) injection for a geometry with a flow barrier.

